Development 136, 4199-4212 (2009) doi:10.1242/dev.040402

Repression of Wasp by JAK/STAT signalling inhibits medial actomyosin network assembly and apical cell constriction in intercalating epithelial cells

Claire Bertet*, Matteo Rauzi and Thomas Lecuit†

Tissue morphogenesis requires stereotyped cell shape changes, such as apical cell constriction in the mesoderm and cell intercalation in the ventrolateral ectoderm of *Drosophila*. Both processes require force generation by an actomyosin network. The subcellular localization of Myosin-II (Myo-II) dictates these different morphogenetic processes. In the intercalating ectoderm Myo-II is mostly cortical, but in the mesoderm Myo-II is concentrated in a medial meshwork. We report that apical constriction is repressed by JAK/STAT signalling in the lateral ectoderm independently of Twist. Inactivation of the JAK/STAT pathway causes germband extension defects because of apical constriction ventrolaterally. This is associated with ectopic recruitment of Myo-II in a medial web, which causes apical cell constriction as shown by laser nanosurgery. Reducing Myo-II levels rescues the JAK/STAT mutant phenotype, whereas overexpression of the Myo-II heavy chain (also known as Zipper), or constitutive activation of its regulatory light chain, does not cause medial accumulation of Myo-II nor apical constriction. Thus, JAK/STAT controls Myo-II localization by additional mechanisms. We show that regulation of actin polymerization by Wasp, but not by Dia, is important in this process. Constitutive activation of Wasp, a branched actin regulator, causes apical cell constriction and promotes medial 'web' formation. Wasp is inactivated at the cell cortex in the germband by JAK/STAT signalling. Lastly, *wasp* mutants rescue the normal cortical enrichment of Myo-II and inhibit apical constriction in JAK/STAT mutants, indicating that Wasp is an effector of JAK/STAT signalling in the germband. We discuss possible models for the role of Wasp activity in the regulation of Myo-II distribution.

KEY WORDS: *Drosophila*, JAK/STAT signalling, Morphogenesis, Apical constriction, Myosin-II, Wasp

INTRODUCTION

During gastrulation, embryonic tissues are shaped following stereotyped patterns. These complex morphogenetic processes require adhesive forces that maintain tissue cohesion, tension generation by myosin motors that drive the remodelling of cell contacts, and cell shape changes. Two main classes of cell morphogenetic processes have been reported. Apical cell constriction is required for local tissue bending and facilitates tissue invagination, such as in the *Drosophila* mesoderm or in vertebrate neural tube closure (Lecuit and Lenne, 2007; Leptin, 2005). In other tissues, cells exchange neighbours during intercalation, and drive convergence and extension movements that elongate the anteroposterior axis (reviewed by Keller, 2006).

Drosophila gastrulation vividly illustrates how tensile forces drive tissue remodelling. During mesoderm invagination, Myosin-II is apically recruited in ventral cells in response to the ligand Fog (Dawes-Hoang et al., 2005). Fog activates RhoGEF2 (Barrett et al., 1997; Hacker and Perrimon, 1998) and the Rho1/Rok1 pathway, and ultimately leads to Myo-II regulatory light chain (MRLC) phosphorylation and activation (reviewed by Tan et al., 1992); MRLC is called Spaghetti Squash (Sqh) in *Drosophila* (Karess et al., 1991). Although it is traditionally thought that apical constriction is driven by circumferential Myo-II at cell junctions, as for instance in vertebrate neurectodermal cells in response to the actin-binding protein Shroom (Hildebrand, 2005), recent studies have shown that constriction in the fly mesoderm is driven by apical medial actomyosin contractility (Martin et al., 2009). Pulses of contractility drive rapid, stepwise cell constriction events. In mesoderm cells, Myo-II is absent from the cortex and accumulates only in a central 'web' at the level of the adherens junctions (AJs).

After mesoderm invagination, ventrolateral (VL) ectodermal cells extend along the anteroposterior (AP) axis in a process called germband extension (GBE) (Bertet et al., 2004; Blankenship et al., 2006; Irvine and Wieschaus, 1994; Zallen and Wieschaus, 2004). GBE is driven by cell intercalation. During this process, cells exchange neighbours by the polarized remodelling of cell contacts. Local Myo-II enrichment leads to increased bond elastic tension and drives changes in cell contacts (Bertet et al., 2004; Rauzi et al., 2008).

This leads to a model in which different regions of the *Drosophila* embryonic epithelium undergo different morphogenetic processes owing to different subcellular regulation of actomyosin network contractility. However, the underlying mechanisms are still poorly understood. First, it is not known what regulates the planar polarized recruitment of Myo-II at the contacts between AP neighbours. More fundamentally, it is not even known what restricts Myo-II at the cortex instead of in the medial apical region in the VL ectoderm.

Myo-II subcelllar localization requires activation by the Rho GTPase and its target Rok, which phosphorylates the MRLC at conserved serine residues (Bertet et al., 2004; Jordan and Karess, 1997; Winter et al., 2001). Rok is the only kinase known to regulate MRLC in flies, although other kinases are likely candidates in other organisms. In conditions that alter MRLC phosphorylation, apical cell constriction is affected (Corrigall et al., 2007; Escudero et al., 2007; Lee and Treisman, 2004). In some cases, active RhoGTP accumulation occurs in regions matching the sites of Myo-II

IBDML, UMR6216 CNRS-Université de la Méditerranée, Campus de Luminy, case 907, 13288 Marseille Cedex 09, France.

*Present address: Department of Biology, New York University, 1009 Silver Center, 100 Washington Square East, New York, NY 10003-6688, USA
†Author for correspondence (lecuit@ibdml.univ-mrs.fr)

Accepted 7 October 2009

enrichment (Bement et al., 2005; Simoes et al., 2006). It has long been assumed that subcellular RhoGTP activation by RhoGEFs or inactivation by RhoGAPs provides the necessary and sufficient molecular signals that determine subcellular localization, especially when Myo-II cortical localization was shown to be independent of actin, such as during cytokinesis (Dean et al., 2005; Kamijo et al., 2006; Zang and Spudich, 1998).

Myo-II binds actin filaments and motor activity drives the movement and dynamics of actin networks. In vivo, actin networks are complex structures. Two types of proteins promote actin filament polymerization. Wasp and Scar, via the regulation of the Arp2/3 complex, promote the polymerization of branched actin filaments (Amann and Pollard, 2001; Pantaloni et al., 2000). The formin Dia promotes the polymerization of non-branched actin filaments (Romero et al., 2004). Non-branched networks facilitate contractility because filaments can move past one another. Indeed, Dia increases Myo-II accumulation at AJs (Homem et al., 2008).

JAK/STAT signalling controls many developmental processes, in particular morphogenetic events involving cell movements (Hou et al., 2002), such as border cell migration in *Drosophila* (Silver et al., 2005; Beccari et al., 2002), prestalk cell movements in *Dictyostelium* (Kawata et al., 1997) or convergence extension movements in the zebrafish (Yamashita et al., 2002). Here, we report that the JAK/STAT signalling pathway is required in early *Drosophila* embryos for germband elongation. We show that JAK/STAT signalling represses actomyosin accumulation in a medial apical 'web' in the VL ectoderm, thus blocking apical constriction in this region of the embryo. Although MRLC (Sqh) phosphorylation by the RhoGEF2/Rho/Rok pathway is necessary for the medial accumulation of Myo-II in JAK/STAT mutants, constitutive activation of Sqh and overexpression of the Myo-II heavy chain (MHC; also known as Zip) do not recapitulate the JAK/STAT mutant phenotype. This suggests that JAK/STAT uses additional mechanisms to control Myo-II recruitment in germband cells. We report that JAK/STAT represses Wasp, and that this is needed to repress the medial web accumulation of Myo-II and cell constriction in the intercalating ectoderm.

MATERIALS AND METHODS

Fly stocks and genetics

Wild-type stocks were *Oregon-R*. Deletion stocks Df(970) and Df(954) were from the Bloomington Stock Center. Mutant alleles used were: upd^{YM55}, hop^{C111} and mrl^{06346} (gift of N. Perrimon, Harvard Medical School, Boston), $eve^{1.27}$ (gift of J. P. Vincent, NIMR, London), $runt^{3}$ (Bloomington), sqh^{AX3} and *sqhE20E21* (gift of R. Karess, Institut Jacques Monod, Paris), $rho1^{K2107B}$, dia^{5} (Bloomington) and $wasp^{3}$ (gift of E. Schejter, Weitzmann Institute, Rehovot).

Time-lapse imaging was performed in *E-cadGFP* (gift of H. Oda, JT Biohistory, Osaka), *sqhAX3; sqhGFP* (gift of R. Karess), *upd/FM7; E-cadGFP* and *upd/FM7;sqhGFP* stocks, and in embryos laid by mothers expressing *E-cadGFP* and in which *hop* germline clones were induced.

Overexpression experiments were done at 18°C, by crossing females expressing *mattubGal4VP16* (67 gal4) with the following UAS lines: *UAS-upd*, *UAS-stat* and *UAS-*hop^{Tuml} (gift of M. Zeidler, University of Sheffield, UK), *UAS-sqhE20E21* (this work), UAS-zipGFP (gift of D. Kiehart, Duke University), *UAS-myr-wasp* (gift of K. Klaembt, Institute für Neurobiologie, Muenster) and *UAS-diaCA NC* (gift of P. Rørth, IMBC, Singapore).

Constructs

The sqhE20E21Flag coding sequence was amplified by PCR from the p-Casper-genomic-sqhE20E21Flag vector (gift of R. Karess) as a *Kpn*I-*Kpn*I fragment and cloned into the pUAST vector. The construct was sequenced before being transformed into flies.

Expression of the construct was checked by RT-PCR on cDNA from embryos laid by 67gal4 females crossed with UASsqhE20E21Flag males, and by western blot using an anti-FLAG antibody (data not shown).

Immunohistochemistry

Embryos were fixed by heat-methanol treatment for stainings with rabbit anti-Zip (1:1000; gift from C. Field, Harvard Medical School, Boston), and mouse anti-Nrt (1:50; Developmental Studies Hybridoma Bank, DSHB). Standard 3.7% formaldehyde (FA) fixation was performed for stainings with rat anti-DE-Cad (1:10; DSHB), mouse anti-Arm/β-cat (1:200; DSHB), rabbit anti-Eve (1:1000; M. Frasch, Friedrich-Alexander University of Erlangen-Nuremberg, Erlangen), guinea pig anti-Runt (1:500; D. Kosman, SUNY, Buffalo), mouse anti-Dia (1:200; S. Wasserman, University of California, San Diego) and rabbit anti-Wasp (1:100; E. Schejter). For Alexa 546-phalloidin (Molecular Probes) labelling, embryos were hand devitellinized.

Injections

Y27632 and Latrunculin-A were injected at the end of cellularization at a concentration of 600 μM and 1 mM, respectively. The dilution factor in the embryo is around 1:50, so we estimated the local concentrations to be 12 μM for Y27632 and 20 μM for Latrunculin-A.

Timelapse analysis and quantifications

Embryos were prepared as detailed by Cavey and Lecuit (Cavey and Lecuit, 2008). Quantifications and statistical tests are detailed below.

Nano-ablation of SqhGFP

We used a home-made set up as described previously (Cavey et al., 2008). Ablation pulses were performed using a 40× water immersion lens NA 1.2, at 370 mW at the back aperture of the objective, for 2.5 milliseconds.

Western blot quantifications

For each genotype, approximately 50 μl of embryos (0-5 hours egg laying collection) were re-suspended in 100 μl of embryo lysis buffer, snap frozen on dry ice, ground, centrifuged for 10 minutes at 25,000 ***g***, and the supernatant then boiled for 10 minutes with 5 μl loading buffer. The following antibodies were used: rabbit anti-Sqh (1:100; Cell Signaling Technology), rabbit anti-Dia (1:5000), rabbit anti-Rho1 (1:20; Cell Signaling Technology) and mouse anti-α-Tub (1:5000; Sigma), which was used as a loading control. Signal detection was performed using an ECL UV imager (Fisher), and quantification of the signal intensity was carried out using the Bio1D software (Vilber Lourmat).

Increasing concentrations of wild-type embryo extracts were used to determine the slope of the ECL signal versus protein concentration. This allowed us to determine how much protein (Sqh, Dia, Rho1 or α-Tub) was present per lane for the different genotypes. Protein levels were then normalized to α-Tub levels.

DIC movies and GBE measurements

Embryos were filmed in phase contrast on a Zeiss microscope with a 20× objective. Time-lapse covered the end of cellularization to the end of germband elongation every 2 minutes. GBE measurements were done at the end of the intercalation process, i.e. 40 minutes after posterior midgut invagination. Percentage of GBE was calculated as the ratio of elongation of the germ band to the maximal elongation in wild-type embryos (cephalic furrow position).

Confocal time-lapse imaging

Embryos were dechorionated with bleach, glued on a coverslip and covered with Halocarbon oil. *upd ;sqhGFP* embryos were filmed with a LSM510 Meta confocal microscope, using an Apochromat 100×/1.4NA objective. Intercalating *cadGFP*, *upd; cadGFP* or *hopGLC;cadGFP* embryos were filmed using a Perkin Elmer spinning disk confocal microscope with a Plan Neo 40×/1.2NA objective. Movies used for measurements were made by projections of *z*-stacks of 1 μm step acquired at 30-second intervals. For each embryo, the surface of 150 cells was measured every 10 minutes, using the Metamorph software.

Quantification of Myo-II distribution and statistical tests

Z-stacks of 0.5 μm step were acquired in fixed embryos stained with anti-Zip and anti-Nrt antibodies. Embryos of different genotypes were fixed en masse, stained with the same antibody solution and processed in parallel. Imaging used the same confocal settings. Bulk amount of Myo-II was measured in the germband at different confocal planes starting from the apical surface to the adherens junctions (step size 0.5 μm). Integrated intensities were calculated in 58×58 μm images using the Metamorph software. Means±s.e.m. of different embryos were calculated. Student's *t*-tests were performed to compare the means between wild-type and mutant embryos.

Apical cell surface measurements and statistical tests

Z-stacks were acquired in fixed embryos stained with anti-Nrt antibody. For each embryo, the apical surface of 40 cells was measured using the Metamorph software. Means±s.e.m. of different embryos were calculated. Student's *t*-tests were performed to compare the means between wild-type and mutant phenotypes.

Cortical/medial Myo-II intensity ratio measurements and statistical tests

Z-stacks were acquired in fixed embryos stained with anti-Zip and anti-Nrt antibodies. Quantifications were performed in the *z*-plane corresponding to the apical side of AJs (500 nm below the apical-most surface). Regions (adherens junctions and apical web) were drawn using Nrt staining and intensity measurements were performed on Zip staining. The mean intensity at adherens junctions (A; cortical) was measured by using the linescan function of the Metamorph software. For each embryo, about 200 junctions were measured. The results were expressed in arbitrary units per pixel and converted to arbitrary units per μm^2 taking into account pixel size for each image. The mean Myo-II intensity in the apical web (B; medial) refers to the average Myo-II integrated intensity per cell normalized to cell surface (expressed in arbitrary unit/μm^2). For each embryo, around 40 apical webs were measured. Finally, the cortical/medial Myo-II intensity ratio was obtained by dividing A by B. For each ratio, standard errors were calculated and Student's *t*-test was performed.

Genotyping live and fixed embryos

All progeny embryos from heterozygous *upd* or *Df* mothers and +/Y fathers were genotyped based on the presence or absence of a GFP marker inserted on an FM7 balancer chromosome. The embryos were laid by mothers Df or *upd/FM7,KrGal4,UASGFP* crossed to males *FM7,KrGal4,UASGFP/Y*. *upd/upd* or *Df/Df* embryos were distinguished from heterozygous embryos based on the absence of GFP scored about 2.5 hours after the onset of gastrulation, at a time when GFP can be easily scored. The presence/absence of GFP and hence genotype was directly associated with a GBE phenotype recorded in time lapse because each embryo had recorded coordinates using a motorized platform and the Mark&Find module from AxioVision software (Zeiss).

For *upd/FM7,KrGal4,UASGFP*, 25/100 embryos had GBE defects and all were *upd/upd*. For *Df/ FM7,KrGal4,UASGFP*, 29 embryos had GBE defects and all were *Df/Df*.

Using the same GFP balancer chromosomes on living embryos expressing an EcadGFP transgene to label cell junctions, we found that all homozygous *upd* mutant embryos displayed characteristic apical cell constriction defects. No single heterozygous *upd* embryo and no *yw* control embryos expressing the same E-cadGFP transgene displayed these defects. For this reason, we used apical cell constriction as a proxy for genotyping *upd* homozygous mutants when embryos were fixed.

Ectopic activation of the JAK/STAT signalling pathway

We overexpressed uniformly different components of the JAK/STAT pathway: *upd*, *stat* and a constitutively active form of JAK, *hopTuml*. Although all the embryos uniformly expressed these transgenes, we found borderline defects with *upd* (13%, *n*=100) and no defects with others (0%, *n*=100). In other contexts, based on the literature, this causes strong gain-of-function defects.

Q-RT-PCR quantifications

Dechorionated embryos were lysed in TRIzol (Invitrogen) and RNAs were prepared according to the manufacturer's protocol and quantified using nanodrop. For each sample, 1 μg of mRNA was reverse-transcribed using oligo-dT-VN primers and ImProm-II as the reverse transcriptase (Promega) in triplicate. Real-time quantitative amplification of RNA (q-PCR) was performed using the Sybr Green qPCR Super Mix (Invitrogen) and the iQ^{TM}5 Real-Time PCR Detection System from BioRad according to the manufacturer's protocol. The relative expression of indicated transcripts was quantified with the iQ5 Optical System Software using the $2^{[-\Delta\Delta C(T)]}$ method. According to this method, the C(T) values for the expression of each transcript in each sample were normalized to the C(T) values of the control mRNA (RP49) in the same sample. The values of untreated cell samples were then set to 100% and the percentage transcript expression was calculated. The results are representative of three independent RT experiments. Primers used in these experiments were:

RP49-F, GACGCTTCAAGGGACAGTATCTG;
RP49-R, AAACGCGGTTCTGCATGAG
Wasp-1188F, ACAGTGTAGAATCCCCTACGG;
Wasp-1584R, GGTTCCCTTGCGTATGG;
Sqh-355F, CCGTGATGGCTTCGTCGAGA; and
Sqh-709R, TTGTCCTTGGCACCGTGCTTA.

RESULTS

JAK/STAT signalling is required for germband extension

In order to identify new zygotic regulators of Myo-II cortical recruitment during GBE, we conducted a genetic screen looking at embryos homozygous mutant for genomic deficiencies. Time-lapse recording of 100 embryos undergoing GBE and quantification of tissue elongation 40 minutes after the onset of GBE (Fig. 1A) identified an important region that is required zygotically for GBE (Fig. 1B, see also Materials and methods). Mutants for *unpaired* (*upd*; *os* – FlyBase), a gene present in this interval and coding for a *Drosophila* ligand of the JAK/STAT signalling pathway (Harrison et al., 1998), display similar defects (see Movies 1 and 2 in the supplementary material): 25% of the progeny of heterozygous upd^{YM55} parents, a null *upd* allele, had these defects and all of them were homozygous mutant, based on in vivo genotyping (see Materials and methods). These defects were rescued following expression of a wild-type *upd* cDNA (see Fig. S1 in the supplementary material; Materials and methods). These defects were noticeably stronger in severity than were those in *eve* mutants, where GBE defects have been previously characterized (Fig. 1C) (Irvine and Wieschaus, 1994).

Upd binds the receptor Domeless (Dome) (Brown et al., 2001), and activates a single JAK kinase called Hopscotch (Hop) (Binari and Perrimon, 1994) and a single STAT transcription factor called Marelle (Mrl/Stat92E) (Hou et al., 1996; Yan et al., 1996) (Fig. 1C). All components of the pathway except for the ligand are maternally provided. Embryos coming from jak/hop^{C111} and $stat/mrl^{06346}$ germline clones (both strong loss-of-function alleles) had GBE defects that were similar to those of *upd* mutants, and were rescued by the zygotic paternal wild-type allele (Fig. 1D).

All components of the JAK/STAT pathway are expressed uniformly prior to GBE, including the ligand Upd. At the onset of GBE, *upd* expression resolves into stripes (Harrison et al., 1998). Uniform activation of the JAK/STAT pathway did not affect GBE and rescued the *upd* mutant phenotypes (see Fig. S1A,B in the supplementary material), suggesting that patterned expression of *upd* might not be essential for GBE (see Materials and methods).

The JAK/STAT signalling pathway regulates the fifth stripe of the pair rule genes *eve* and *runt* (Binari and Perrimon, 1994; Harrison et al., 1998; Hou et al., 1996), both of which are also required for GBE

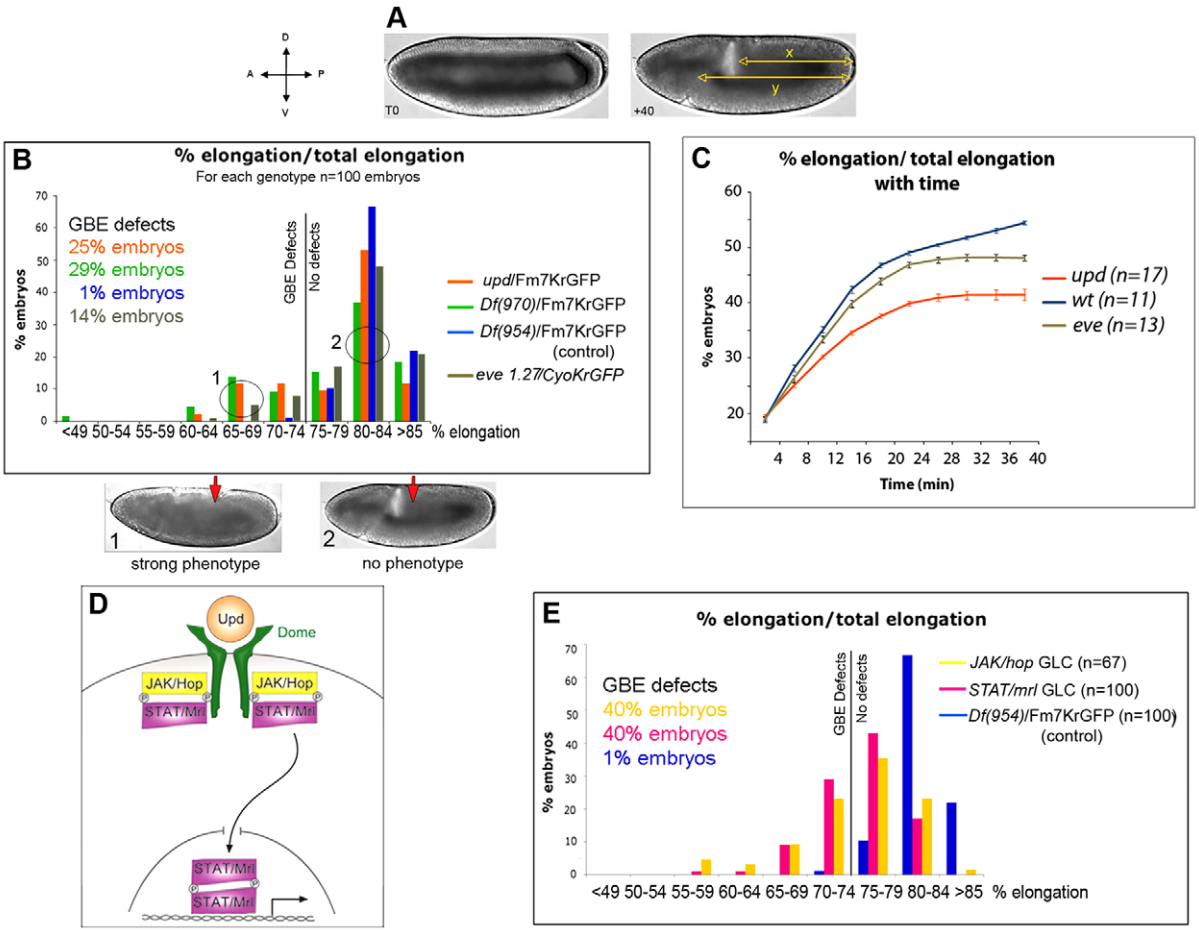

Fig. 1. JAK/STAT signalling is required for germband extension. (**A**) Scheme for GBE measurements, showing an embryo at t0 (onset of GBE) and t=40 minutes (end of intercalation). The percentage of GBE is calculated as the ratio of elongation of the germ band after 40 minutes (arrow, *x*) to the maximal elongation (arrow, *y*). (**B**) Histogram of GBE in 100 embryos each from parents heterozygous for Df(970) removing the *upd* locus (green), for *upd* (orange), for a control deficiency (Df*954*, blue) and for *eve* null mutants (grey). Embryos were classified as having GBE defects if their elongation was <75% that of wild type (see vertical line); the percentage of embryos showing GBE defects in each group is indicated on the top left corner. Images of embryos with strong GBE defects (circle 1) and wild-type GBE (circle 2) are shown below (red arrows indicate the extent of elongation at t=40 minutes). (**C**) GBE temporal evolution in *upd* mutants (orange), wild type (*wt*, blue) and *eve* (grey) mutants. GBE defects start very early in *upd* mutants and are stronger than those observed in *eve* mutants. Error bars indicate s.e.m. (**D**) Schematic of the JAK/STAT signalling pathway. (**E**) Distribution of GBE in 100 embryos each from *JAK/hop* (yellow) and *STAT/mrl* (pink) germline clones and the control Df*954* deficiency stock (blue).

(Irvine and Wieschaus, 1994). This suggested that *JAK/STAT* signalling could control GBE via the pair rule genes *eve* and *runt*. However, although the cuticle patterning defect was fully penetrant in *jak/hop* mutants (see Fig. S2A,A′ in the supplementary material), we failed to detect any obvious and penetrant defects in Eve and Runt expression during GBE (0 defects in 21 embryos laid by *hop* germline clone mothers; see Fig. S2B,C in the supplementary material), suggesting that the reported obvious loss of *eve* and *runt* stripe 5 might not be very penetrant (Binari and Perrimon, 1994; Harrison et al., 1998; Hou et al., 1996). This suggests that JAK/STAT signalling controls GBE independently of *eve* and *runt*. This is confirmed by the fact that cell shape defects observed in *upd* mutants (see below) are not observed in *eve* and *runt* mutants (data not shown).

Abnormal apical cell constriction in JAK/STAT mutants

We next addressed the cellular basis of GBE defects observed in JAK/STAT mutants. In JAK/STAT pathway mutants, although epithelial cells in the head and dorsal-most regions were normal, intercalating (ventrolateral) cells displayed a smaller apical surface than did controls at the same stage (Fig. 2A,B). Time-lapse imaging of *upd* mutant embryos expressing the fusion protein E-Cad::GFP showed that this was due to neither ectopic cell divisions (normally repressed at this stage), nor cell delamination (as is the case when junctions collapse), but was the result of an ectopic apical cell constriction (Fig. 2C,D; see also Movies 3 and 4 in the supplementary material). This defect was fully penetrant in *upd* hemizygotes (see Materials and methods) and in *jak/hop* mutants (data not shown). We quantified changes in the apical cell surface over time: in contrast to wild-type controls where the surface is nearly constant, in *upd* and *jak/hop* mutants the apical cell surface decreased gradually and became conspicuous when intercalation normally starts (Fig. 2E). At the end of GBE, the apical cross section area was reduced by 40% in *upd* mutants compared with in wild-type controls. In addition to apical cell constrictions, *upd* mutants exhibited cell intercalation defects, which were variable in strength (see Fig. S3 in the supplementary material). In the most extreme cases, cell intercalation was blocked (Fig. 2F and see Fig. S3 in the

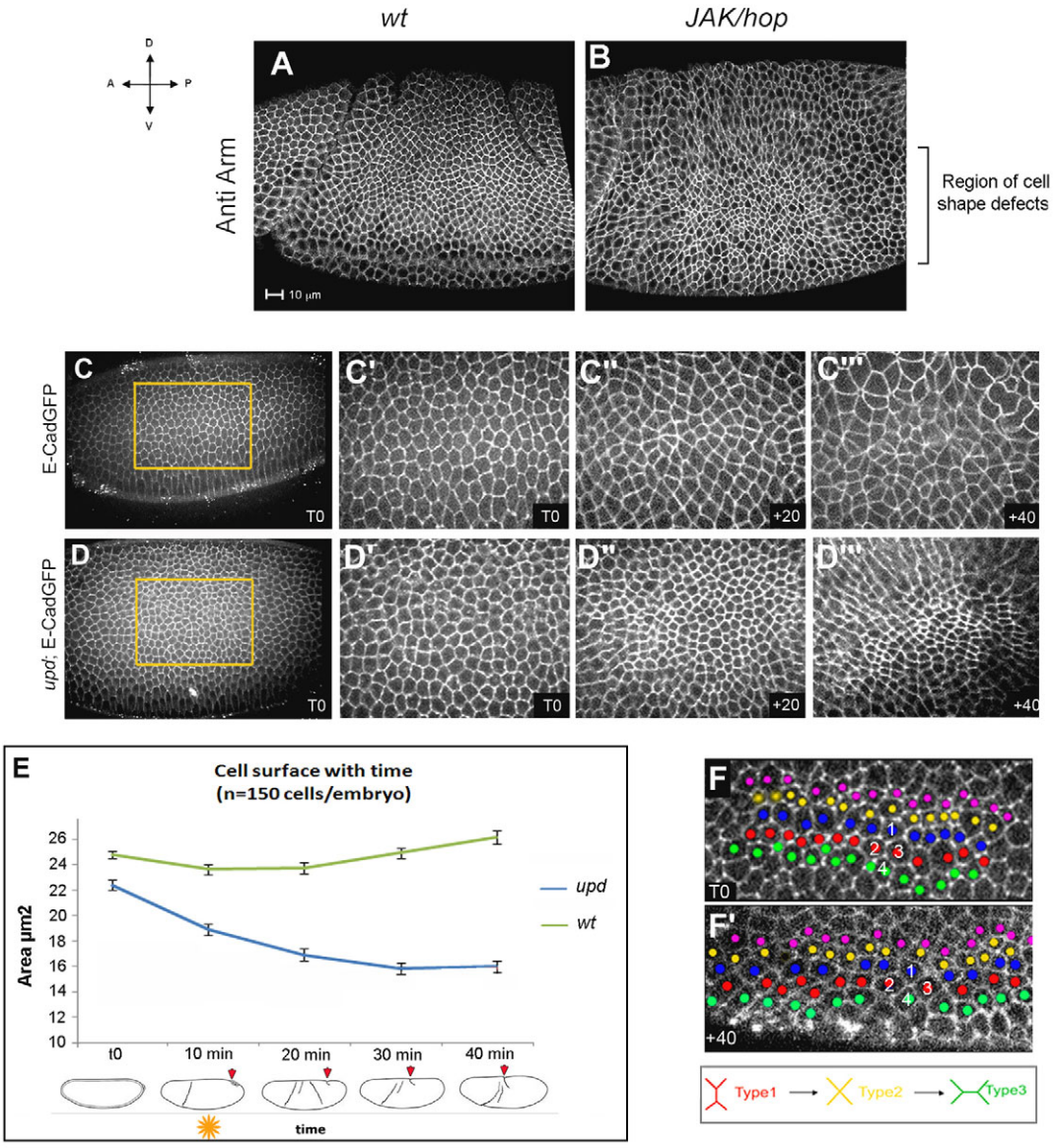

Fig. 2. Abnormal apical cell constriction in JAK/STAT pathway mutants. (**A**,**B**) Antibody staining for Arm/βcat showing a smaller apical surface in intercalating cells of *JAK/hop* embryos (B) compared with wild type (*wt*, A). (**C-D‴**) Time-lapse confocal sequences of cells in the VL region (rectangles in C,D) of E-cad::GFP (C-C‴) and *upd*; E-cadGFP (D-D‴) embryos over a 40-minute period. Note the smaller apical cell surface in *upd* mutants. (**E**) Quantification of apical cell surface changes over time in *wt* (green) and *upd* (blue) mutant embryos. T0 marks the end of cellularization, cell intercalation starts at t=10 minutes (orange star). Schematics under the graph indicate elongation of the germband at each time point (red arrows). Error bars indicate s.e.m. Apical constriction in JAK/STAT mutants begins at T0, and persists later. (**F**,**F′**) Strong cell intercalation defects in *JAK/hop*; E-CadGFP embryos. Intercalating cells are colored with dots and tracked over time. Some cells do intercalate (e.g. cells 1 and 4) but the majority does not.

supplementary material). Thus, ectopic apical cell constriction and associated defects in cell intercalation provide a simple explanation for the failure to extend the germband.

Medial Myo-II accumulation causes apical constriction

These results point directly to potential defects in Myo-II localization in JAK/STAT pathway mutants. In control embryos, Myo-II is mainly localized at the apical cortex of intercalating cells (Fig. 3A-A″). In JAK/STAT pathway mutants, Myo-II is strongly enriched apically in a more medial position (Fig. 3B-B″,C-C″; see also Fig. S4A,B in the supplementary material) compared with in wild type (Fig. 3A-A″). Closer examination indicates a significant enrichment both at the AJs and within 1 µm apically of the AJs (Fig. 3E-E″, compare with Fig. 3D-D″; quantification in Fig. 3F, $P<1\times10^{-4}$). Besides the overall increase of Myo-II in the apical region of intercalating cells, a striking feature was a change in the subcellular localization of the actomyosin network. We measured the medial to cortical Myo-II ratio at the apical extent of AJs (500 nm below the apical-most region, see Materials and methods) in wild type and *upd* mutants. Whereas Myo-II is mostly cortical in wild type with only very low levels in the apical medial region (Fig. 3D-D″), in *upd* mutants (Fig. 3E-E″) Myo-II is strongly enriched in a medial meshwork, such that the ratio between cortical and medial Myo-II is significantly reduced compared with in wild type ($P<6\times10^{-5}$; Fig. 3G,H).

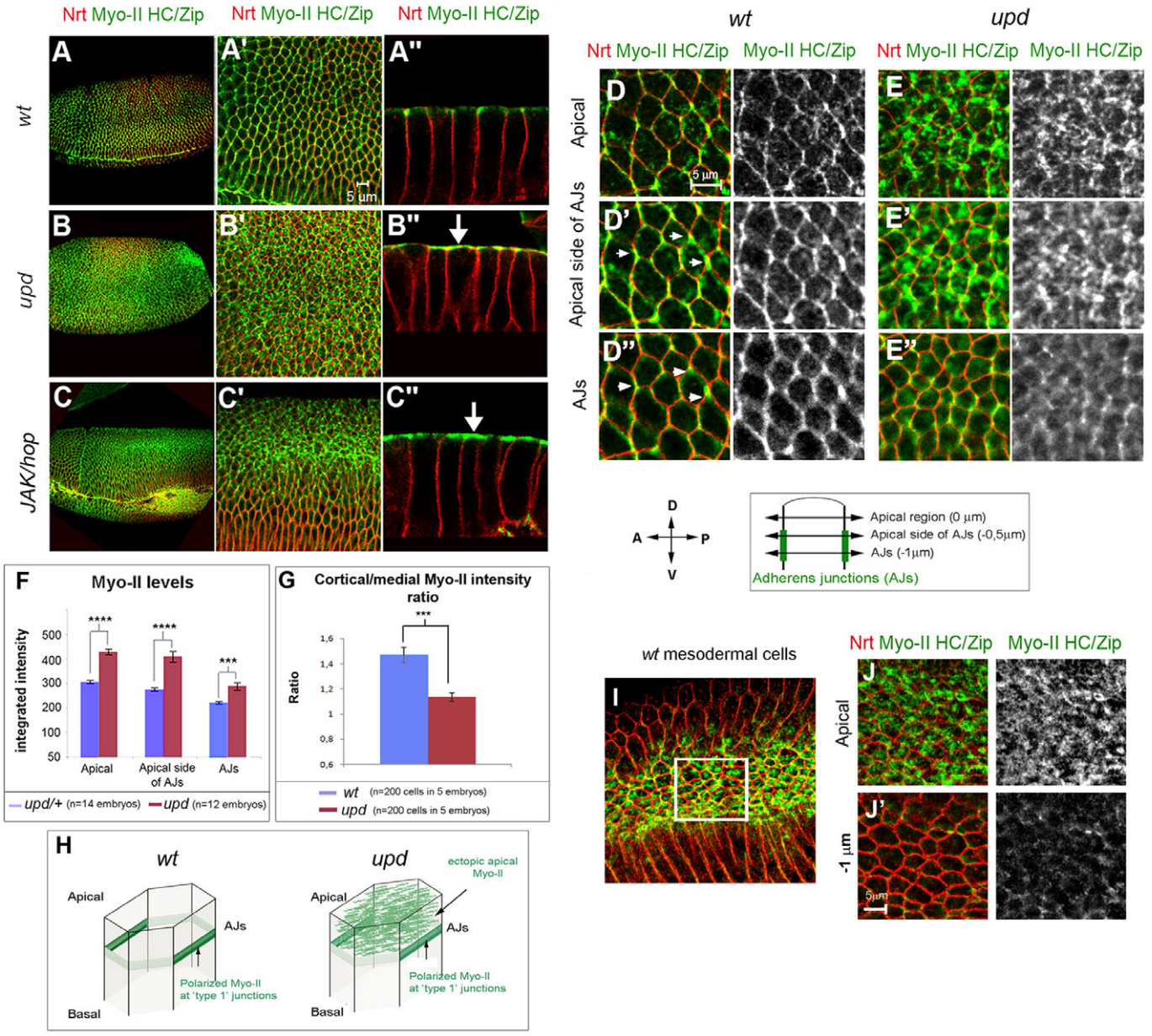

Fig. 3. Ectopic medial apical accumulation of Myo-II in JAK/STAT mutants. (**A-E″**) Antibody staining for MHC (Zip, green) and the membrane marker Neurotactin (Nrt, red) in wild type (*wt*, A-A″), *upd* (B-B″) and *JAK/hop* embryos (C-C″) in whole mounts (A-C), apical sections (A′,B′,C′) and sagittal views (A″,B″,C″), showing ectopic enrichment of Myo-II apically in *JAK/hop* and *upd* mutants (arrow in B″,C″). *z*-stacks at higher magnification in *wt* (D-D″) and *upd* mutants (E-E″) show that in *wt* embryos Myo-II is concentrated at AJs, where it is polarized at type 1 junctions (arrows in D″). In *upd* mutants, Myo-II is highly enriched in the apical-most region of intercalating cells and within the apical extent of AJs. (**F**) Quantification of Myo-II (*y*-axis) in different *z*-planes (*x*-axis, see scheme) in *upd* heterozygous (*upd*/+, blue) and *upd* homozygous (*upd*, red) mutants. Student's *t*-test: $***P<1\times10^{-4}$, $****P<1\times10^{-5}$. (**G**) Cortical to medial Myo-II intensity ratio in *wt* (blue) and *upd* homozygous mutants (*upd*, red). In *upd* mutants, Myo-II is strongly enriched in the medial apical web, leading to a significant decrease of the ratio. Student's *t*-test: $****P<6\times10^{-5}$. (**H**) Summary of Myo-II recruitment defects in JAK/STAT mutants compared to *wt*. (**I-J′**) Antibody staining for MHC (Zip, green) and the membrane marker Neurotactin (Nrt, red) in the presumptive mesodermal cells of a *wt* embryo. In these cells, Myo-II is strongly enriched in an apical web (J) and seems to be excluded from adherens junctions (J′). Error bars indicate s.e.m.

Using a *MRLC/sqh::GFP* transgene, we found that the ectopic apical recruitment of Myo-II is detected just after cellularisation, preceding conspicuous apical constriction (see Fig. S4C,D in the supplementary material). Ectopic MRLC/Sqh::GFP is not cytoplasmic but is present on very dynamic structures, most likely actin fibers underlying the apical surface (see Movie 5 in the supplementary material; compare with Movie 6). In JAK/STAT pathway mutants, Myo-II is thus apically recruited prematurely, and in excess in a medial apical 'web' (Fig. 3H). This situation is reminiscent of the mesoderm cells, although an important difference is that Myo-II is still present at the cortex in *upd* mutants, whereas it is only present in a medial apical web in the mesoderm (Martin et al., 2009) (Fig. 3I,J). This resemblance with mesodermal cells strongly suggests that, in JAK/STAT mutants,

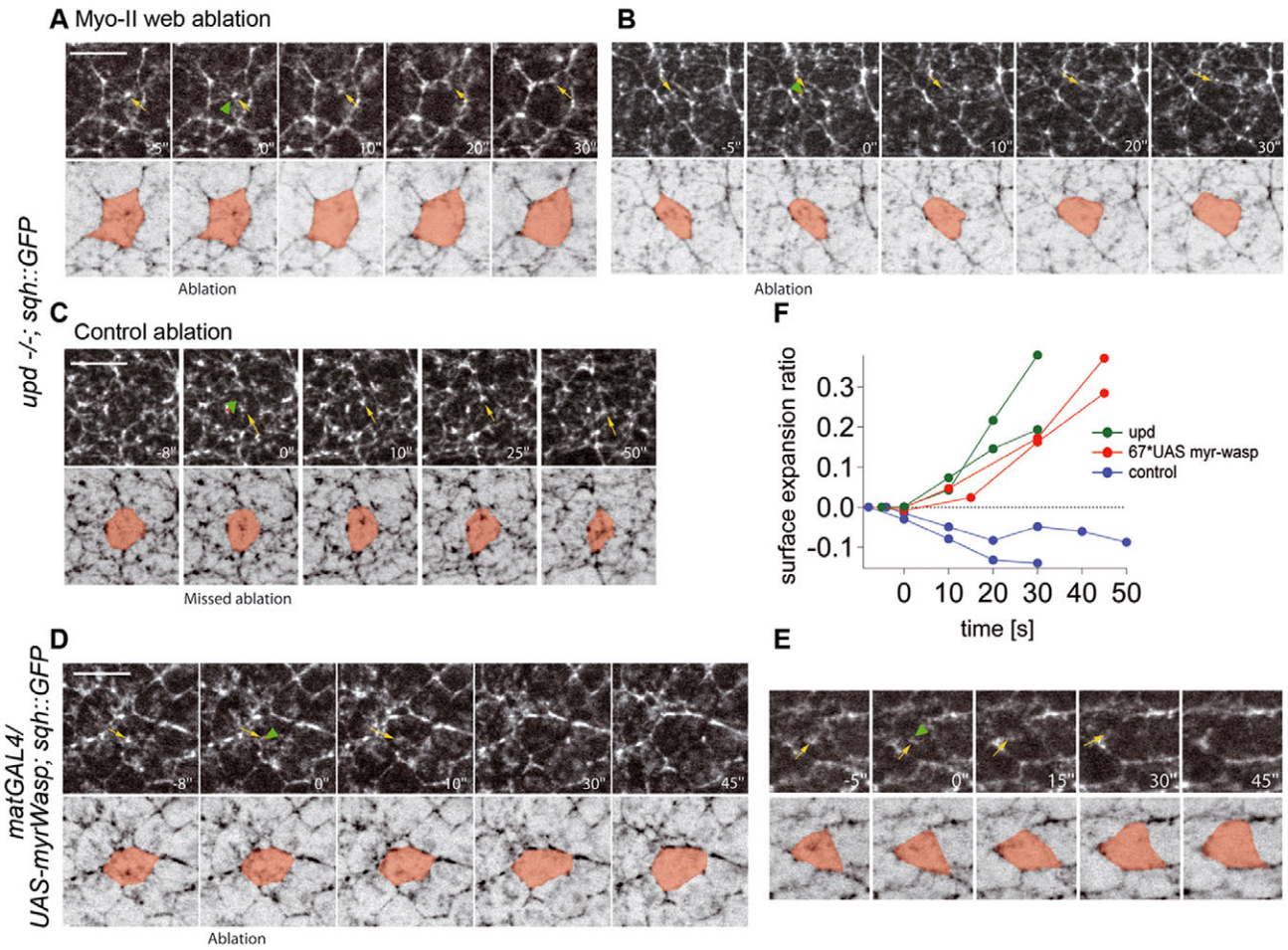

Fig. 4. Severing of medial apical Myo-II web causes apical surface relaxation. (**A-E**) Time-lapse confocal images of embryos expressing SqhGFP in *upd* mutants (A-C) or expressing *myrWasp* (D,E), before and after focal ablation (green arrowhead) with a pulsed infrared laser in a diffraction limited spot (~200 nm) for 2.5 milliseconds. Targeting ablation on SqhGFP medial clusters in *upd* mutants caused area relaxation together with redistribution of SqhGFP (yellow arrows). The normalized area relaxation was stronger when constriction was greater (compare A and B). Ablation in the medial region using similar parameters but away from SqhGFP clusters did not cause area relaxation (C). Similar observations were made in *myrWasp*-expressing embryos (D,E). (**F**) Quantification of area relaxation ratio as a function of time.

the ectopic medial apical Myo-II pool might be responsible for ectopic apical cell constriction in germband cells. In order to test this directly, we performed focal ablation of the medial Myo-II 'web' with nano-scissors, a pulsed near IR-laser beam focused on a diffraction-limited spot (200-300 nm) for 2-3 milliseconds (see Rauzi et al., 2008). This led to the fragmentation of the medial actomyosin meshwork and to its redistribution away from the ablation points towards the cortex (Fig. 4A, yellow arrows). Importantly, this was also accompanied by a progressive relaxation of the apical cell surface within 30 seconds (Fig. 4A,B). When constriction was weak at the onset of ablation, the cell surface relaxed more modestly with a change in the curvature of the boundaries (Fig. 4A,F; see also Movie 7 in the supplementary material). The effects were stronger when constriction was more prominent (38% surface relaxation, Fig. 4B,F; see Movie 8 in the supplementary material) and were commensurate with apical surface constriction in *upd* mutants (–40%). Laser pulses outside of the apical Myo-II medial clusters did not cause Myo-II redistribution, nor area relaxation (Fig. 4C,F; see Movie 9 in the supplementary material), indicating that relaxation requires the ablation of tensile elements in the medial region. Together, these observations indicate that ectopic medial Myo-II is responsible for the abnormal cell constriction observed in *upd* mutants.

To test whether efforts to elongate the germband might affect non-autonomous Myo-II accumulation in the germband, we knocked down *Krüppel* by RNAi in *upd* embryos. GBE was strongly reduced in *Krüppel* RNAi embryos (data not shown), and Myo-II polarized accumulation at the cortex was severely perturbed in all embryos (see Movie 10 in the supplementary material). RNAi of *Krüppel* did not affect the penetrance of medial Myo-II accumulation in *upd* mutants (30%, n=23) and the defects were indistinguishable from those of *upd* mutants alone (see Movie 11 in the supplementary material). This suggests that Myo-II localization defects are likely to be cell autonomous.

Increased Myo-II levels and activation are necessary but not sufficient to promote apical constriction

Myo-II is present overall at higher levels apically in *upd* mutants (40% increase compared with wild type). Western blot analysis confirms this finding (Sqh levels are 20% higher in *hopGLC* in which 60% of

embryos show GBE defects, compared with in wild type, not shown). This raises the question of whether elevated levels of Myo-II are necessary and sufficient to produce the changes in actomyosin localization and cell constriction in JAK/STAT pathway mutants. To test whether Myo-II levels are necessary for the aberrant apical constriction, we performed genetic epistasis experiments between *upd* and a protein null allele of *sqh* (*sqh*^{AX3}). Western blotting indicated that embryos laid by heterozygous *upd, sqh*/+ parents had on average a 38±9% reduction in Sqh compared with embryos laid by *upd*/+ parents (Fig. 5A, inset). This reduction of Sqh levels was sufficient to rescue the GBE defects normally observed in *upd* mutants (Fig. 5A, 24% defects in the progeny of *upd* heteterozygous parents compared with 4.5% on average within the progeny of *upd, sqh*^{AX3} heterozygous parents). Indeed, apical cell constriction was significantly rescued in *upd, sqhZ/Z,M*/+ embryos [i.e. embryos removing the zygotic (Z) contribution of *sqh* and half of its maternal (M) contribution] compared with in *upd* mutants (Fig. 5B, n=200 cells in 5 embryos, $P<6\times10^{-16}$). Consistent with this, together with the expected globally reduced amount of Myo-II (Fig. 5C-E), the ratio between cortical and medial Myo-II was restored and similar to in wild type (Fig. 5F).

Heterozygosity for *rho1*, required for the activation of MRLC (Sqh) via Rok, also rescues the GBE phenotype of *upd* mutants (see Fig. S5A-C in the supplementary material; 24% and 6% defects in the progeny of, respectively, *upd* and *upd, rho1*/+ heterozygous parents). Rho1 is on average reduced by 60±9% in embryos coming from *upd*/+ and *rho1*/+ parents compared with those from *upd*/+ parents (Fig. S5A, inset). Injection of low concentrations of the Rok inhibitor Y-27632 into *hop* mutants also partially reduced the penetrance of the GBE defects observed compared with water-injected controls (37% compared with 75% GBE defects, respectively; Fig. S5D in the supplementary material). Thus, Myo-II activation is necessary for the ectopic apical constriction in *upd* mutants.

To test whether upregulation of Myo-II is sufficient to generate *upd* mutant phenotypes, we overexpressed MHC (Zip) or SqhE20E21, a phosphomimetic form of Sqh that renders it constitutively active (Winter et al., 2001). Ubiquitous expression of SqhE20E21 at similar levels to endogenous Sqh expression (not shown) using the *sqh* promotor (called endoSqhE20E21) rescued the phenotype of embryos injected with a Rok inhibitor, which removes endogenous Sqh from the cortex (Bertet et al., 2004). Additionally SqhE20E21 expression further enhanced the GBE defects in *upd* mutants (Fig. S5E in the supplementary material), clearly indicating that SqhE20E21 is active. In either case, GBE defects were not observed (Fig. 6A), despite a marked increase in the total levels of MHC (Zip) at the apical cell region when Zip was overexpressed, or upon overexpression of SqhE20E21 (Fig. 5B-D). In both cases, apical enrichment of MHC was significant (P<0.001 for ZipGFP and P<0.02 for SqhE20E21, Fig. 6E), although it was less pronounced in the case of SqhE20E21. Finally, we found that neither Zip nor SqhE20E21 overexpression induced apical cell constriction (Fig. 6F), and that the overexpression of these genes generated a relative increase in cortical Myo-II compared with the medial apical

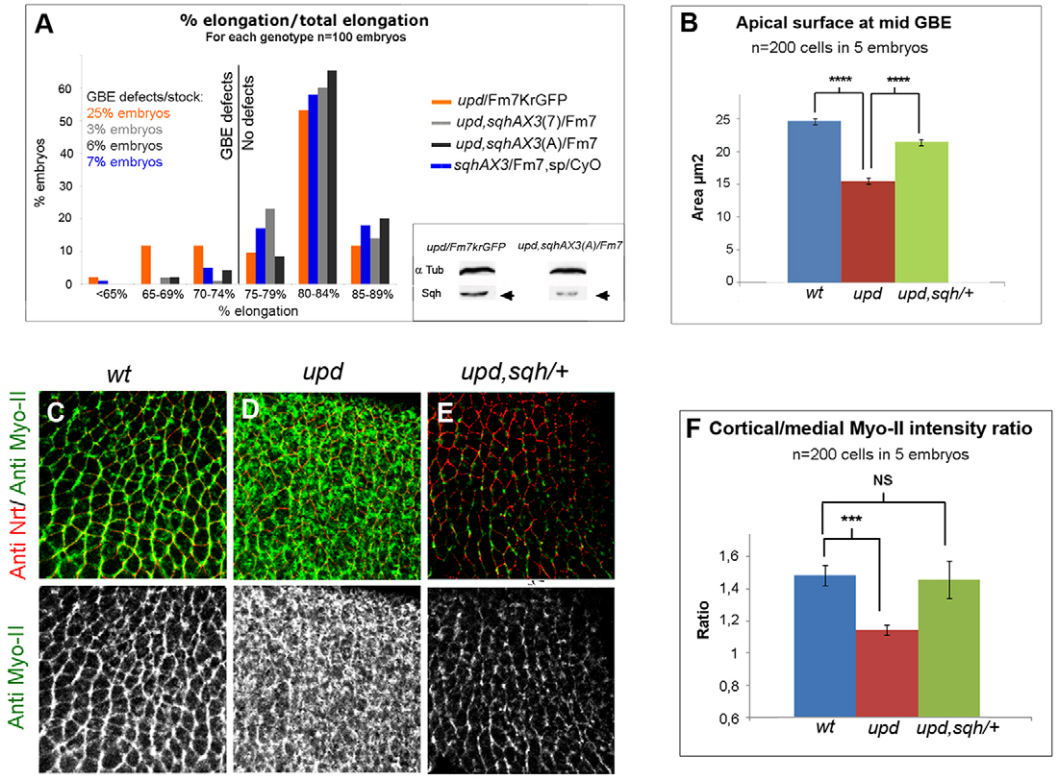

Fig. 5. Myo-II mediates the role of JAK/STAT in morphogenesis. (**A**) Histogram of GBE in the progeny of *upd*/+ (orange) and *sqh*^{AX3}/+ (blue) parents and in two independent *upd,sqh*^{AX3}/+ recombinants (grey) in which the defects are rescued. Inset shows western blot quantifications of Sqh, which is reduced by 40% in embryos laid by *upd,sqh*^{AX3}/+ parents. (**B**) Apical cell surface at mid GBE in *wt* (blue), *upd* (red) and *upd,sqh*^{AX3}/+ (green) embryos. Ectopic apical cell constriction defects are rescued in *upd,sqh*^{AX3}/+ embryos. Student's *t*-tests: between *wt* and *upd*, ****$P<6\times10^{-32}$; between *upd* and *upd,sqh*^{AX3}/+, ****$P<6\times10^{-16}$. (**C-E**) Antibody stainings for MHC (Zip, green) and the membrane marker Neurotactin (Nrt, red) in *wt* (C), *upd* (D) and *upd,sqh*^{AX3}/+ embryos (E), showing that Myo-II ectopic recruitment is rescued in *upd,sqh*^{AX3}/+ embryos. (**F**) Cortical to medial Myo-II intensity ratio. Removing amounts of Sqh in *upd* mutants (green) restores a *wt* ratio. Students *t*-tests: between *upd* and *wt*, ***$P<6\times10^{-4}$; between *wt* and *upd,sqh*^{AX3}/+, P<0.4 (not significant). Error bars indicate s.e.m.

web pool (Fig. 6G; $P<1.5\times10^{-3}$ for ZipGFP and $P<0.04$ for SqhE20E21). This Myo-II cortical enrichment is the opposite of that observed in *upd* mutants.

Altogether these results lead us to conclude that although Myo-II is upregulated in *upd* mutants and is required to mediate apical constriction, neither its concentration, nor its activation by Rok are sufficient to explain the formation of a medial apical meshwork and the associated changes in cell shape. This suggests that JAK/STAT signalling controls Myo-II subcellular localization via additional mechanisms.

Different roles of Wasp and Dia in the formation of a medial or cortical actomyosin network

Despite several reports that, at least during cytokinesis, Myo-II cortical enrichment is independent of F-actin (Dean et al., 2005; Kamijo et al., 2006; Zang and Spudich, 1998), Myo-II co-localized with F-actin in the apical region of intercalating cells (see Fig. S6A in the supplementary material) and disappeared from regions of the cortex where F-actin was removed upon depolymerization by Latrunculin-A (Fig. S6A,B in the supplementary material). Thus, during GBE, junctional Myo-II requires its binding to F-actin.

This led us to test the role of regulators of actin polymerization in the control of Myo-II recruitment. We first tested the role of actin polymerization controlled by the formin Dia (Fig. 7A). We overexpressed a constitutively active form of Dia, Dia^{CA} (Somogyi and Rorth, 2004), that localizes to the apical cell cortex (Fig. 7B). In this situation, Myo-II was increased apically, consistent with previous reports (Homem and Peifer, 2008) (Fig. 7D,F, $P<0.004$), but the ratio of cortical to medial Myo-II was not significantly altered (Fig. 7H). Consistent with this, in embryos laid by *dia*/+ mothers, in which *dia* is on average reduced by 65±7% (mean±s.e.m., Fig. S6B in the supplementary material) compared with wild-type controls, Myo-II levels were decreased and the cortex/medial web ratio was unaffected (Fig. 7H, $P<0.1$, not

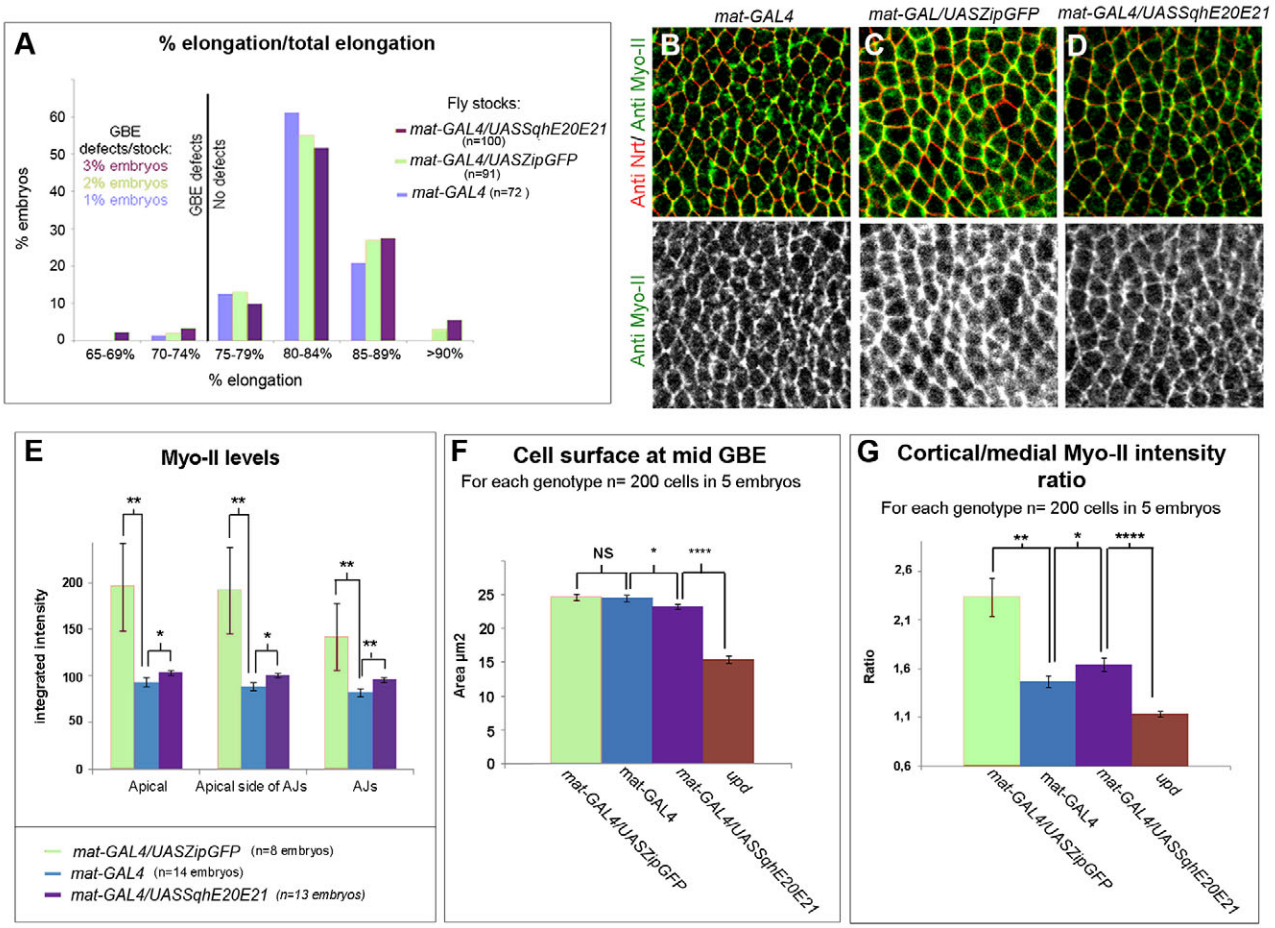

Fig. 6. Increased Myo-II levels and activation are necessary but not sufficient to promote apical constriction. (**A**) Histogram of GBE in the progeny of 67Gal4 controls (blue), 67Gal4/UAS-*sqhE20E21* females crossed to *UAS-sqhE20E21* males (purple) and 67Gal4/*UAS-zip::GFP* females crossed with *UAS-zipGFP* males (pink). Increasing the levels of Myo-II protein or activation does not generate GBE defects. (**B-D**) Distribution of MHC (Zip, green) and Nrt (red) at the level of the apical side of AJs of embryos laid by 67Gal4 controls (B), 67Gal4/UAS-*sqhE20E21* females crossed to *UAS-sqhE20E21* males (C), 67Gal4/*UAS-zip::GFP* females crossed with *UAS-zipGFP* males (D). Myo-II cortical recruitment is increased upon overexpression of sqhE20E21 or Zip. (**E**) Quantification of Myo-II levels at different *z*-planes. In all planes, Myo-II levels are higher upon overexpression of sqhE20E21 (purple; Student's *t*-tests: $*P<0.047$, 0.021 and 0.005, respectively) or Zip (pink; $**P<0.0017$, 0.0012 and 0.0097, respectively). (**F**) Apical cell surface at mid GBE. Overexpression of Zip does not generate ectopic apical constriction (orange, Student's *t*-test, $P<0.41$, not significant). Overexpression of SqhE20E21 generates a slight decrease of apical cell surface (purple, 22.98±0.41 µm^2 compared with 24.21±0.44 µm^2 in 67Gal4; Student's *t*-test: $*P<0.031$. (**G**) Cortical to medial Myo-II intensity ratio. SqhE20E21 (purple) and Zip (pink) overexpression lead to a significant increase of the ratio, indicating an enrichment of Myo-II at the cell cortex. Student's *t*-test: between 67Gal4 and 67Gal4/*UASsqhE2021*, $*P<0.04$; between 67Gal4 and 67Gal4/*UASZipGFP*, $**P<1.5\times10^{-3}$. Error bars indicate s.e.m.

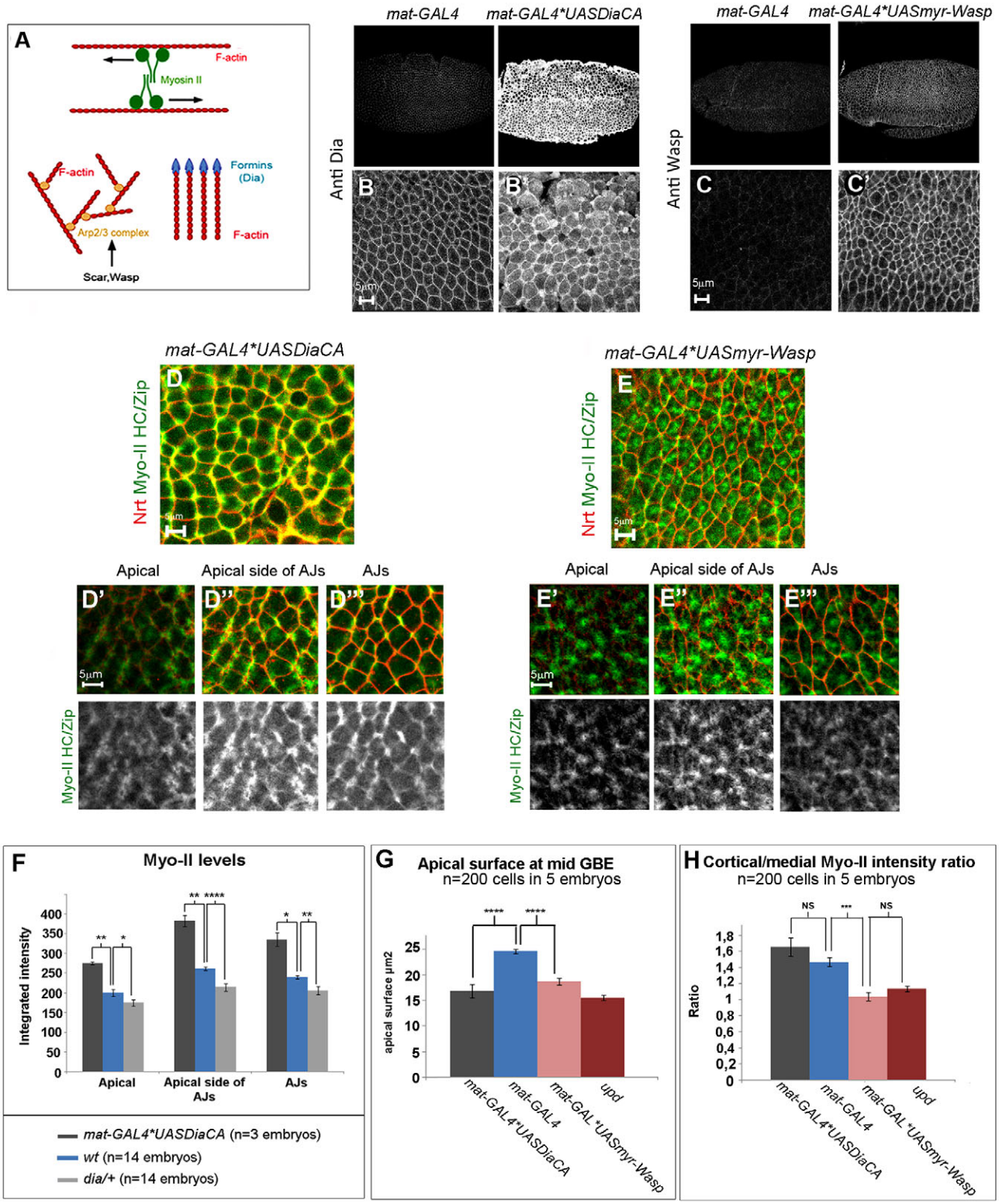

Fig. 7. See next page for legend.

significant; see Fig. S6C,D in the supplementary material). Dia^{CA} led to a collapse of the epithelium, which explains the apical cell surface reduction observed in these embryos (Fig. 7G, $P<7\times10^{-22}$). Thus, Dia-dependent actin polymerization is required to regulate the amount of Myo-II recruited in apical actin networks.

Testing the role of actin polylmerization by Wasp led to a very different result. We first expressed a myristoylated form of Wasp (myr-Wasp) (Bogdan et al., 2004; Bogdan et al., 2005), which strongly targets Wasp to the plasma membrane (Fig. 7C). In mammalian cells Wasp is normally recruited and activated at the

Fig. 7. Opposite effects of Wasp and Dia on the formation of a medial or cortical actomyosin network. (**A**) Summary of the two main modes of actin polymerization. (**B-C′**) Antibody staining against actin cytoskeleton regulators. (B,B′) Anti-Dia staining in *wt* (B) and in 67Gal4**UAS DiaCA* (B′) embryos, showing a strong accumulation of Dia at the cell cortex of 67Gal4**UAS DiaCA* embryos. (C,C′). Anti-Wasp staining in *wt* (C) and 67Gal4**UAS myr-Wasp* (C′) embryos, showing a strong accumulation of Wasp at the cell cortex of *67*UAS myr-Wasp* embryos. (**D-E‴**) Antibody staining for MHC (Zip, green) and Neurotactin (Nrt, red) in different *z*-planes of 67Gal4**UAS DiaCA* (D-D‴) and 67Gal4**UAS myr-Wasp* (E-E‴) embryos. Myo-II is strongly enriched at the cell cortex of 67Gal4**UAS DiaCA* embryos, whereas it is excluded from the cortex of 67Gal4**UAS myr-Wasp* embryos. (**F**) Quantification of Myo-II levels in different *z*-planes in *wt* (blue), 67Gal4**UAS DiaCA* (dark grey) and embryos laid by *dia*/+ parents (clear grey). Overexpressing DiaCA leads to an enrichment of Myo-II in all planes (Student's *t*-tests: $^{**}P<0.004$, $^{**}4.5\times10^{-3}$ and *0.013, respectively), whereas removing Dia leads to a decrease of Myo-II levels in all planes (Student's *t*-test: $^{*}P<0.016$, $^{****}5.4\times10^{-5}$ and **0.003, respectively). (**G**) Apical cell surface at mid GBE in 67Gal4 (blue), 67Gal4**UAS DiaCA* (grey), 67Gal4**UAS myr-Wasp* (pink) and *upd* (red). Overexpression of DiaCA or myr-Wasp generates ectopic apical constriction (Student's *t*-tests: $^{****}P<7\times10^{-22}$ for DiaCA and $^{****}P<4\times10^{-12}$ for myr-Wasp). (**H**) Cortical to medial Myo-II intensity ratio. The ratio is unchanged in UASDiasCA (grey) compared with *67Gal4* (blue, $P<0.1$, not significant), whereas it strongly decreases in UASmyr-Wasp embryos (pink, $P<6\times10^{-4}$) in the same manner as in *upd* mutants (red, $P<0.07$, not significant).

plasma membrane by Cdc42, although in flies, binding to Cdc42 can be dispensable (Tal et al., 2002). The myristoylated group bypasses this regulatory mechanism and leads to constitutive activation at the plasma membrane. Interestingly, not only did this fail to increase Myo-II at the cortex, but Myo-II strongly accumulated in a medial network (Fig. 7E, $P<6\times10^{-4}$; see also Fig. 7H, and Movie 12 in the supplementary material), although it was still present, albeit at low levels, at the cortex. This led to ectopic apical constriction (Fig. 7G, 28% surface area reduction, $P<4\times10^{-12}$). Focal ablation in a diffraction limited spot for 2-3 milliseconds of the medial Myo-II web led to Myo-II redistribution at the cortex together with surface area relaxation (Fig. 4D-F; see also Movie 12 in the supplementary material), suggesting that, as for *upd* mutants, medial Myo-II accumulation in myrWasp-expressing embryos causes apical constriction. Wasp was shown not to be essential for viability at early stages of development (Ben-Yaacov et al., 2001). Consistent with this, we could not reveal a role of Wasp during GBE (not shown). This can be simply explained by the fact that, as shown below, Wasp activation is normally downregulated specifically in the germband.

Together these data reveal a central role of actin polymerization in the control of Myo-II cortical or medial localization. They also indicate different roles for Dia and Wasp in the regulation of Myo-II localization. Dia controls the total amount of Myo-II present apically in both the cortex and the medial web, but up- or down-regulation of Dia does not affect the ratio between the cortex and the medial web. However, activation of Wasp has a strong impact on this ratio and leads to cell constriction. Moreover, these data show that Wasp activation bears strong similarities with *upd* inactivation, in that it causes both apical constriction and medial accumulation of Myo-II.

Repression of Wasp by JAK/STAT is required for cortical Myo-II concentration

This led us to investigate whether JAK/STAT controls Myo-II apical medial recruitment by inhibiting Wasp. We first investigated the localization of Wasp. In wild-type embryos, Wasp was detected at the apical cell cortex at the end of cellularisation and in early gastrulating embryos during mesoderm invagination. However, at the onset of GBE, the levels of Wasp at the cell cortex dropped, especially in the VL intercalating regions where Myo-II was largely cortical. Wasp was still detected more dorsally at the cortex (Fig. 8A). Thus, Wasp was no longer detected and presumably was not activated at the cell cortex in intercalating cells. This downregulation of Wasp required JAK/STAT signalling. Indeed, in *hop* mutants, at the onset of GBE, Wasp was still strongly enriched at the apical cell cortex in the VL regions of the embryo, where cells undergo abnormal apical constriction (Fig. 8B). Thus, JAK/STAT signalling downregulates the cortical recruitment of Wasp in intercalating cells.

In order to understand how JAK/STAT regulates the cortical localization of Wasp, we performed quantitative RT-PCR experiments. These experiments revealed that the levels of *wasp* transcripts were the same in wild type and in *hop* mutants (data not shown). We conclude that the JAK/STAT signalling pathway does not repress the cortical recruitment of Wasp by regulating *wasp* transcription, but presumably by as yet unknown post-transcriptional mechanisms.

To test whether Wasp overactivation is required to mediate Myo-II medial accumulation in JAK/STAT mutants and apical constriction, we performed an epistasis experiment. We investigated whether a reduction in *wasp* gene dosage rescues apical constriction and the medial accumulation of Myo-II observed in *upd* mutants (Fig. 8C-E). As shown in Fig. 8E, the characteristic medial apical accumulation of Myo-II in *upd* mutants was lost in *upd* mutant embryos laid by mothers heterozygous for a null allele of *wasp*, $wasp^{3}$. The global enrichment of Myo-II apically was similar in *upd* mutants and *upd; $wasp^{3}$/+* mutants (Fig. 8F, $P>0.05$), but the cortical/medial Myo-II ratio was rescued in *upd; $wasp^{3}$/+* mutants, with significantly more Myo-II at the cortex (Fig. 8G, $P<0.006$). This was accompanied by a rescue of the apical constriction phenotype (Fig. 8H, $P>0.05$). We conclude that, at the onset of GBE, the JAK/STAT signalling pathway represses Wasp activation. This repression is essential to prevent medial Myo-II accumulation and promotes the enrichment of Myo-II at the cortex, which is characteristic of intercalating cells. Note that Myo-II cortical localization is not totally normal in *upd; wasp/+* mutant embryos; its planar polarized distribution is affected (Fig. 8E). Consistent with this, GBE extension is defective in these double mutants.

DISCUSSION

Myo-II subcellular localization controls different cell shape changes such as cell constriction or intercalation. The data we report shed new light on the mechanisms of the subcellular localization of actomyosin networks in the early *Drosophila* ectoderm. VL ectodermal cells intercalate via the cortical recruitment of Myo-II at AJs, which drives polarized junction remodelling (Bertet et al., 2004; Blankenship et al., 2006; Rauzi et al., 2008). This contrasts with the behaviour of immediately adjacent cells in the mesoderm, which undergo apical constriction and recruit Myo-II into a medial apical web (Martin et al., 2009). Our data indicate that the cortical enrichment of Myo-II in ectodermal intercalating cells is not a 'default pathway', and requires at least activity of the JAK/STAT

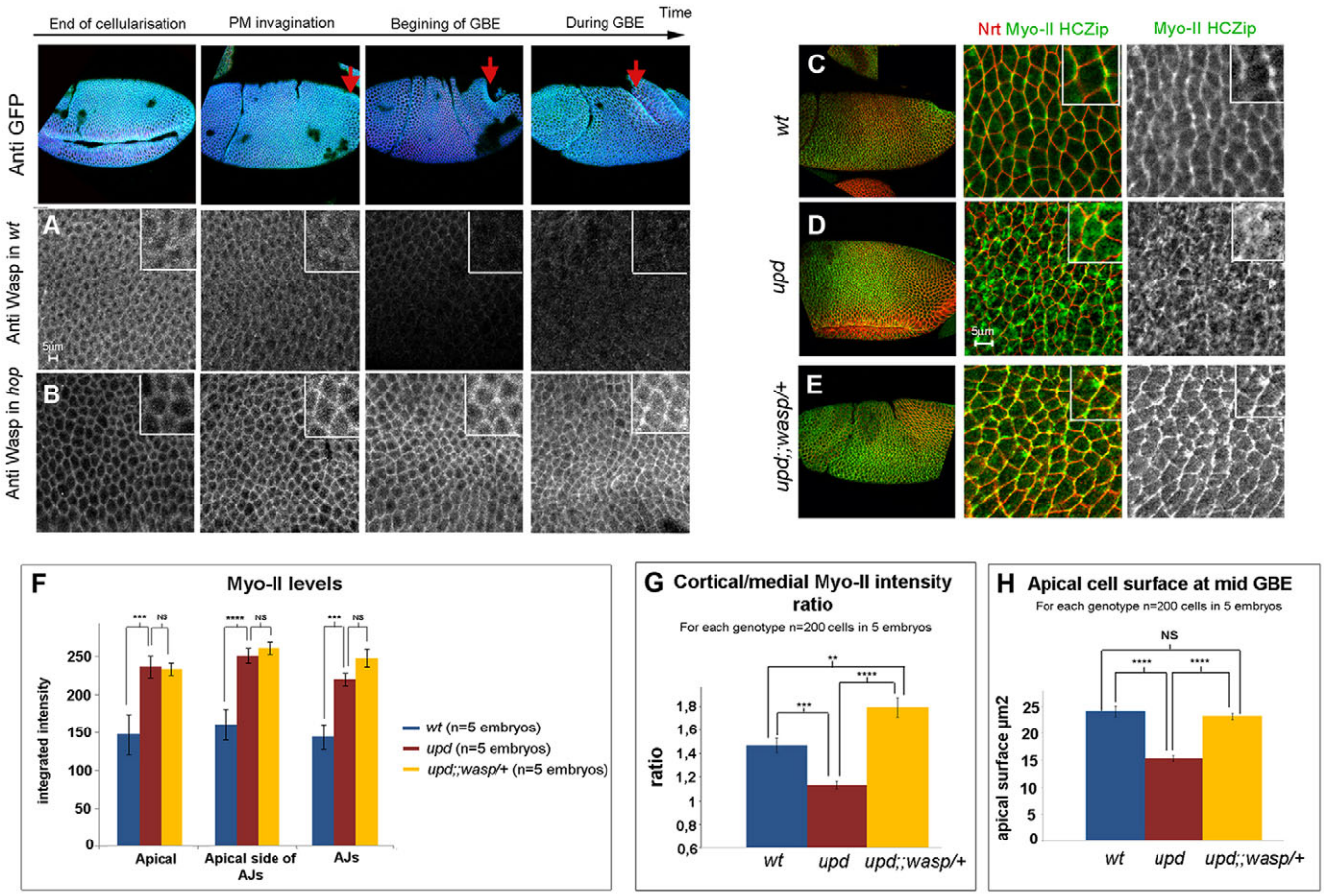

Fig. 8. Repression of Wasp by JAK/STAT is required for cortical Myo-II concentration. (**A**,**B**) Antibody staining against Wasp (green), Nrt (red) and GFP (blue) in *wt* (A) and *hop* mutants (B), showing that Wasp is ectopically recruited at AJs in *hop* mutants during GBE. (**C-E**) Localization of MHC (Zip, green) and Nrt (red) in *wt* (C), *upd* (D), and *upd; wasp* (E) embryos. Myo-II cortical recruitment is enhanced in *upd; wasp* embryos compared with in *upd* single mutants, and planar polarity is disrupted. (**F**) Quantification of Myo-II levels in different *z*-planes in *wt* (blue), *upd* (red) and *upd; wasp/+* (yellow) embryos. Reducing Wasp in *upd* mutants does not rescue Myo-II ectopic apical recruitment [Student's *t*-tests between *upd* and *upd; wasp/+*: $P<0.4$ (not significant), $P<0.3$ (not significant) and $P<0.06$ (not significant), respectively]. (**G**) Cortical/medial Myo-II intensity ratio. The ratio is significantly increased in *upd; wasp/+* embryos (yellow) compared with in *upd* mutants (red) or in *wt* (blue), indicating an enrichment of Myo-II at the cell cortex and thus a rescue of the *upd* phenotype (Student *t*-tests: between *wt* and *upd; wasp/+*, $**P<0.006$; and between *upd* and *upd; wasp/+*, $****P<3.2\times10^{-5}$. (**H**) Apical cell surface measurements at mid GBE. Ectopic apical constriction is rescued in *upd; wasp/+* embryos [Student's *t*-test between *wt* and *upd; wasp/+*, $P<0.11$ (not significant)].

pathway. Indeed, in JAK/STAT pathway mutants, Myo-II is aberrantly recruited in a medial apical meshwork and cells consequently undergo apical constriction. This is surprising, as apical constriction is normally only observed in mesodermal ventral cells and is considered to be a unique attribute owing to their selective expression of Twist and Snail. Twist and Snail induce expression of the ligand Fog in the ventral cells only, which activates RhoGEF2, Rok and Myo-II. It also regulates expression of the transmembrane protein T48, which participates in the apical recruitment of RhoGEF2 and contributes to apical constriction (Kolsch et al., 2007). However it is not clear whether activation of the RhoGEF2 pathway is sufficient to drive the apical medial recruitment of Myo-II (Martin et al., 2009). Here, we show that apical constriction is not simply induced in mesodermal cells by Fog, but is also prevented in ectodermal cells by activity of the JAK/STAT pathway and that this is essential for GBE. In JAK/STAT pathway mutants, ectodermal cells undergo apical constriction despite the absence of ectopic Twist expression (see Fig. S7 in the supplementary material). Note, however, that apical constriction is not as rapid in these mutants as in mesodermal cells, so Twist and Snail accelerate or render more efficient the capacity to apically constrict. Moreover, the fact that Wasp mediates JAK/STAT function in the ectoderm but is not required in the mesoderm indicates that the mechanisms promoting medial Myo-II in mesoderm cells are likely to be different.

Our findings provide a novel opportunity to investigate the regulation of cortical or medial Myo-II localization in the ectoderm. Our data document two novel features of this regulation.

MRLC (Sqh) phosphorylation by the RhoGEF2 and the Rok pathway are both necessary for apical constriction, as lowering the dose of RhoGEF2, Rho or Rok suppress the apical constriction observed in *upd* mutants. However, neither constitutive activation of this pathway by expression of a phosphomimetic form of Sqh, ShqE20E21, which rescues Rok inhibition (Bertet et al., 2004), nor overexpression of MHC (Zip) is sufficient to promote medial accumulation of Myo-II. The medial accumulation of Myo-II requires additional regulation apart from the activation of Myo-II. As RhoGEF2 and Rok are key regulators of Myo-II, this

suggests that activation of the RhoGEF2/Rok pathway is necessary but not sufficient to explain medial Myo-II accumulation and apical constriction.

Our analysis of the JAK/STAT mutant phenotypes indicates a key role of Wasp in this process. Wasp is shown to be necessary for medial Myo-II accumulation, at least in ectodermal cells, and very strong activation of Wasp at the cortex (myrWasp) also causes medial Myo-II accumulation (Fig. 6). Moreover, although Wasp is normally downregulated in VL ectodermal cells, in JAK/STAT pathway mutants Wasp is strongly recruited and hence activated at the plasma membrane, which suggests that JAK/STAT signalling represses the membrane activation of Wasp. Importantly, lowering the dose of Wasp maternally suppresses medial accumulation of Myo-II in *upd* mutants, and restores prominent accumulation at the cortex, as in wild-type embryos. Consistent with this, ectopic apical constriction is completely rescued in these double mutant embryos.

We report two different roles for Dia and Wasp in the regulation of Myo-II localization. Consistent with previous data, Dia controls the amount of apical Myo-II, but the specific localization of Myo-II at the cortex or in the medial network is not affected by loss of Dia. Dia promotes polymerization of non-branched filaments, and might control the formation of a good substrate for the stable association of Myo-II minifilaments. The fact that in *dia* heterozygotes the amount of apical Myo-II is reduced indicates that the amount of actin filaments might be limiting and controlled. Indeed, more F-actin is detected at the cortex of intercalating cells, preceding by a few minutes the enrichment of Myo-II (Blankenship et al., 2006). The role of Wasp is more surprising and unique, as it is shown to mediate specifically repression of medial Myo-II accumulation and, hence, cell constriction in the germband. Because activation of Wasp leads to activation of medial web formation and reduction of Wasp dosage rescues cortical Myo-II in JAK/STAT mutants, we conclude that Wasp controls an essential feature of Myo-II subcellular localization that is essential for the regulation of apical constriction. How does Wasp control Myo-II localization? We can envisage two non-exclusive models. In the first model, Wasp controls actin branching through activation of the Arp2/3 complex (Ben-Yaacov et al., 2001). Because Wasp has been implicated in endocytosis via Arp2/3 in *Drosophila* (Georgiou et al., 2008; Leibfried et al., 2008), Wasp could promote Myo-II web formation indirectly by regulating endocytosis of a surface protein required to anchor the medial actomyosin network at the membrane, such as E-cadherin. Consistent with this, downregulation of E-cadherin by RNAi disrupts the faint medial Myo-II pool (M.R., unpublished). In mesodermal cells, E-cadherin appears to anchor the strong medial Myo-II pool (Dawes-Hoang et al., 2005; Martin et al., 2009). In the second model, Wasp might act more directly via the regulation of actin network architecture and its impact on the dynamic interactions between the medial web and the cortex, and thereby might affect the steady-state distribution of Myo-II exchanging between these two pools. Although Wasp uniquely mediates Myo-II regulation via JAK/STAT in the ectoderm and not in the mesoderm, regulation of Arp2/3 might be more generally implicated in the control of Myo-II regulation.

Although *wasp* is an important mediator of JAK/STAT function in the ectoderm, it is unlikely to be the only one. Indeed *wasp* mutants rescue the cortical accumulation of Myo-II and apical constriction in *upd* mutants, but GBE is still strongly affected (data not shown); we noticed that cortical Myo-II distribution was not properly polarized in the plane of the epithelium. This suggests that other subcellular processes are also perturbed in the mutant. The fact that a reduction of Myo-II levels suppresses the *upd* defects indicates that the overall dosage of Myo-II is important as well. Identifying the transcriptional targets of JAK/STAT might shed light on its complex regulatory role during embryonic morphogenesis.

Finally, although this work identifies an important regulator of Myo-II network subcellular distribution in epithelial cells, it is still not clear what regulates the polarized distribution of Myo-II at the cortex.

JAK/STAT signalling controls a number of developmental processes. Importantly, this pathway has been implicated in diverse morphogenetic processes, such as convergent extension movements in the zebrafish embryo, hindgut elongation in *Drosophila* embryos, which probably involves intercalation movements as well (Johansen et al., 2003), and posterior spiracle morphogenesis in *Drosophila* embryos (Sotillos et al., 2008). JAK/STAT signalling also controls border cell migration (Beccari et al., 2002; Brown et al., 2006; Ghiglione et al., 2002; Silver et al., 2005). Our data indicate that JAK/STAT signalling plays an important and hitherto unappreciated morphogenetic function in gastrulating embryos. We document that, JAK/STAT controls, via Wasp, a morphogenetic switch based on the regulation of medial or cortical Myo-II distribution. Interestingly, dorsal cells do not undergo apical constriction in JAK/STAT mutants. Indeed, dorsal cells exhibit neither cortical nor medial web Myo-II and are thus unable to participate in profound tissue remodelling. It appears that DV patterning provides a first general subdivision within the embryonic epithelium whereby Myo-II is globally repressed dorsally, and activated laterally and ventrally. Cortical or medial web distribution then results from the combinatorial input of Fog and JAK/STAT.

Acknowledgements

We thank Jean-Marc Philippe for performing the QRT-PCR experiments and Ahmed Fatmi and Virginie Thomé for assistance. We are grateful to all those who generously provided us with reagents, especially C. Field for the gift of Zipper antibody at a crucial time, and E. Schejter, M. Zeidler, S. Wasseman, N. Perrimon, R. Karess, D. Kiehart, K. Klaembt, P. Rørth, H. Oda, J. P. Vincent, A. Gautreau, M. Frash, D. Kosma and the Bloomington Stock Center. We thank the members of the Lecuit lab for fruitful discussions, as well as S. Kerridge, M. Cavey, S. Merabet, B. Charroux and P. F. Lenne for useful comments on the manuscript. This work was supported by the CNRS, the ACI-BCMS (Ministère de la recherche), the Association pour la Recherche sur la Cancer (ARC), the Fondation Schlumberger pour l'Education et la Recherche (FSER), and the EMBO Young Investigator Programme. C.B. was the recipient of a fellowship from the ARC.

Supplementary material

Supplementary material for this article is available at
http://dev.biologists.org/cgi/content/full/136/24/4199/DC1

References

Amann, K. J. and Pollard, T. D. (2001). The Arp2/3 complex nucleates actin filament branches from the sides of pre-existing filaments. *Nat. Cell Biol.* **3**, 306-310.

Barrett, K., Leptin, M. and Settleman, J. (1997). The Rho GTPase and a putative RhoGEF mediate a signaling pathway for the cell shape changes in Drosophila gastrulation. *Cell* **91**, 905-915.

Beccari, S., Teixeira, L. and Rorth, P. (2002). The JAK/STAT pathway is required for border cell migration during Drosophila oogenesis. *Mech. Dev.* **111**, 115-123.

Bement, W. M., Benink, H. A. and von Dassow, G. (2005). A microtubule-dependent zone of active RhoA during cleavage plane specification. *J. Cell Biol.* **170**, 91-101.

Ben-Yaacov, S., Le Borgne, R., Abramson, I., Schweisguth, F. and Schejter, E. D. (2001). Wasp, the Drosophila Wiskott-Aldrich syndrome gene homologue, is required for cell fate decisions mediated by Notch signaling. *J. Cell Biol.* **152**, 1-13.

Bertet, C., Sulak, L. and Lecuit, T. (2004). Myosin-dependent junction remodelling controls planar cell intercalation and axis elongation. *Nature* **429**, 667-671.

Binari, R. and Perrimon, N. (1994). Stripe-specific regulation of pair-rule genes by hopscotch, a putative Jak family tyrosine kinase in Drosophila. *Genes Dev.* **8**, 300-312.

Blankenship, J. T., Backovic, S. T., Sanny, J. S., Weitz, O. and Zallen, J. A. (2006). Multicellular rosette formation links planar cell polarity to tissue morphogenesis. *Dev. Cell* **11**, 459-470.
Bogdan, S., Grewe, O., Strunk, M., Mertens, A. and Klambt, C. (2004). Sra-1 interacts with Kette and Wasp and is required for neuronal and bristle development in Drosophila. *Development* **131**, 3981-3989.
Bogdan, S., Stephan, R., Lobke, C., Mertens, A. and Klambt, C. (2005). Abi activates WASP to promote sensory organ development. *Nat. Cell Biol.* **7**, 977-984.
Brown, S., Hu, N. and Hombria, J. C. (2001). Identification of the first invertebrate interleukin JAK/STAT receptor, the Drosophila gene domeless. *Curr. Biol.* **11**, 1700-1705.
Brown, S., Zeidler, M. P. and Hombria, J. E. (2006). JAK/STAT signalling in Drosophila controls cell motility during germ cell migration. *Dev. Dyn.* **235**, 958-966.
Cavey, M., Rauzi, M., Lenne, P. F. and Lecuit, T. (2008). A two-tiered mechanism for stabilization and immobilization of E-cadherin. *Nature* **453**, 751-756.
Corrigall, D., Walther, R. F., Rodriguez, L., Fichelson, P. and Pichaud, F. (2007). Hedgehog signaling is a principal inducer of Myosin-II-driven cell ingression in Drosophila epithelia. *Dev. Cell* **13**, 730-742.
Dawes-Hoang, R. E., Parmar, K. M., Christiansen, A. E., Phelps, C. B., Brand, A. H. and Wieschaus, E. F. (2005). folded gastrulation, cell shape change and the control of myosin localization. *Development* **132**, 4165-4178.
Dean, S. O., Rogers, S. L., Stuurman, N., Vale, R. D. and Spudich, J. A. (2005). Distinct pathways control recruitment and maintenance of myosin II at the cleavage furrow during cytokinesis. *Proc. Natl. Acad. Sci. USA* **102**, 13473-13478.
Escudero, L. M., Bischoff, M. and Freeman, M. (2007). Myosin II regulates complex cellular arrangement and epithelial architecture in Drosophila. *Dev. Cell* **13**, 717-729.
Georgiou, M., Marinari, E., Burden, J. and Baum, B. (2008). Cdc42, Par6, and aPKC regulate Arp2/3-mediated endocytosis to control local adherens junction stability. *Curr. Biol.* **18**, 1631-1638.
Ghiglione, C., Devergne, O., Georgenthum, E., Carballes, F., Medioni, C., Cerezo, D. and Noselli, S. (2002). The Drosophila cytokine receptor Domeless controls border cell migration and epithelial polarization during oogenesis. *Development* **129**, 5437-5447.
Hacker, U. and Perrimon, N. (1998). DRhoGEF2 encodes a member of the Dbl family of oncogenes and controls cell shape changes during gastrulation in Drosophila. *Genes Dev.* **12**, 274-284.
Harrison, D. A., McCoon, P. E., Binari, R., Gilman, M. and Perrimon, N. (1998). Drosophila unpaired encodes a secreted protein that activates the JAK signaling pathway. *Genes Dev.* **12**, 3252-3263.
Hildebrand, J. D. (2005). Shroom regulates epithelial cell shape via the apical positioning of an actomyosin network. *J. Cell Sci.* **118**, 5191-5203.
Homem, C. C. and Peifer, M. (2008). Diaphanous regulates myosin and adherens junctions to control cell contractility and protrusive behavior during morphogenesis. *Development* **135**, 1005-1018.
Hou, S. X., Zheng, Z., Chen, X. and Perrimon, N. (2002). The Jak/STAT pathway in model organisms: emerging roles in cell movement. *Dev. Cell* **3**, 765-778.
Hou, X. S., Melnick, M. B. and Perrimon, N. (1996). Marelle acts downstream of the Drosophila HOP/JAK kinase and encodes a protein similar to the mammalian STATs. *Cell* **84**, 411-419.
Irvine, K. D. and Wieschaus, E. (1994). Cell intercalation during Drosophila germband extension and its regulation by pair-rule segmentation genes. *Development* **120**, 827-841.
Johansen, K. A., Iwaki, D. D. and Lengyel, J. A. (2003). Localized JAK/STAT signaling is required for oriented cell rearrangement in a tubular epithelium. *Development* **130**, 135-145.
Jordan, P. and Karess, R. (1997). Myosin light chain-activating phosphorylation sites are required for oogenesis in Drosophila. *J. Cell Biol.* **139**, 1805-1819.
Kamijo, K., Ohara, N., Abe, M., Uchimura, T., Hosoya, H., Lee, J. S. and Miki, T. (2006). Dissecting the role of Rho-mediated signaling in contractile ring formation. *Mol. Biol. Cell* **17**, 43-55.
Karess, R. E., Chang, X. J., Edwards, K. A., Kulkarni, S., Aguilera, I. and Kiehart, D. P. (1991). The regulatory light chain of nonmuscle myosin is encoded by spaghetti- squash, a gene required for cytokinesis in Drosophila. *Cell* **65**, 1177-1189.
Kawata, T., Shevchenko, A., Fukuzawa, M., Jermyn, K. A., Totty, N. F., Zhukovskaya, N. V., Sterling, A. E., Mann, M. and Williams, J. G. (1997). SH2 signaling in a lower eukaryote: a STAT protein that regulates stalk cell differentiation in dictyostelium. *Cell* **89**, 909-916.
Keller, R. (2006). Mechanisms of elongation in embryogenesis. *Development* **133**, 2291-2302.
Kolsch, V., Seher, T., Fernandez-Ballester, G. J., Serrano, L. and Leptin, M. (2007). Control of Drosophila gastrulation by apical localization of adherens junctions and RhoGEF2. *Science* **315**, 384-386.
Lecuit, T. and Lenne, P. F. (2007). Cell surface mechanics and the control of cell shape, tissue patterns and morphogenesis. *Nat. Rev. Mol. Cell Biol.* **8**, 633-644.
Lee, A. and Treisman, J. E. (2004). Excessive myosin activity in mbs mutants causes photoreceptor movement out of the Drosophila eye disc epithelium. *Mol. Biol. Cell* **15**, 3285-3295.
Leibfried, A., Fricke, R., Morgan, M. J., Bogdan, S. and Bellaiche, Y. (2008). Drosophila Cip4 and WASp define a branch of the Cdc42-Par6-aPKC pathway regulating E-cadherin endocytosis. *Curr. Biol.* **18**, 1639-1648.
Leptin, M. (2005). Gastrulation movements: the logic and the nuts and bolts. *Dev. Cell* **8**, 305-320.
Martin, A. C., Kaschube, M. and Wieschaus, E. F. (2009). Pulsed contractions of an actin-myosin network drive apical constriction. *Nature* **457**, 495-499.
Pantaloni, D., Boujemaa, R., Didry, D., Gounon, P. and Carlier, M. F. (2000). The Arp2/3 complex branches filament barbed ends: functional antagonism with capping proteins. *Nat. Cell Biol.* **2**, 385-391.
Rauzi, M., Verant, P., Lecuit, T. and Lenne, P. F. (2008). Nature and anisotropy of cortical forces orienting Drosophila tissue morphogenesis. *Nat. Cell Biol.* **10**, 1401-1410.
Romero, S., Le Clainche, C., Didry, D., Egile, C., Pantaloni, D. and Carlier, M. F. (2004). Formin is a processive motor that requires profilin to accelerate actin assembly and associated ATP hydrolysis. *Cell* **119**, 419-429.
Silver, D. L., Geisbrecht, E. R. and Montell, D. J. (2005). Requirement for JAK/STAT signaling throughout border cell migration in Drosophila. *Development* **132**, 3483-3492.
Simoes, S., Denholm, B., Azevedo, D., Sotillos, S., Martin, P., Skaer, H., Hombria, J. C. and Jacinto, A. (2006). Compartmentalisation of Rho regulators directs cell invagination during tissue morphogenesis. *Development* **133**, 4257-4267.
Somogyi, K. and Rorth, P. (2004). Evidence for tension-based regulation of Drosophila MAL and SRF during invasive cell migration. *Dev. Cell* **7**, 85-93.
Sotillos, S., Diaz-Meco, M. T., Moscat, J. and Castelli-Gair Hombria, J. (2008). Polarized subcellular localization of Jak/STAT components is required for efficient signaling. *Curr. Biol.* **18**, 624-629.
Tal, T., Vaizel-Ohayon, D. and Schejter, E. D. (2002). Conserved interactions with cytoskeletal but not signaling elements are an essential aspect of Drosophila WASp function. *Dev. Biol.* **2**, 260-271.
Tan, J. L., Ravid, S. and Spudich, J. A. (1992). Control of nonmuscle myosins by phosphorylation. *Annu. Rev. Biochem.* **61**, 721-759.
Winter, C. G., Wang, B., Ballew, A., Royou, A., Karess, R., Axelrod, J. D. and Luo, L. (2001). Drosophila Rho-associated kinase (Drok) links Frizzled-mediated planar cell polarity signaling to the actin cytoskeleton. *Cell* **105**, 81-91.
Yamashita, S., Miyagi, C., Carmany-Rampey, A., Shimizu, T., Fujii, R., Schier, A. F. and Hirano, T. (2002). Stat3 Controls Cell Movements during Zebrafish Gastrulation. *Dev. Cell* **2**, 363-375.
Yan, R., Small, S., Desplan, C., Dearolf, C. R. and Darnell, J. E., Jr (1996). Identification of a Stat gene that functions in Drosophila development. *Cell* **84**, 421-430.
Zallen, J. A. and Wieschaus, E. (2004). Patterned gene expression directs bipolar planar polarity in Drosophila. *Dev. Cell* **6**, 343-355.
Zang, J. H. and Spudich, J. A. (1998). Myosin II localization during cytokinesis occurs by a mechanism that does not require its motor domain. *Proc. Natl. Acad. Sci. USA* **95**, 13652-13657.